

Carbon-Nanotube-Based Materials for Protein Crystallization

Piyapong Asanithi,[†] Emmanuel Saridakis,[‡] Lata Govada,[§] Izabela Jurewicz,[†] Eric W. Brunner,[†] Rajesh Ponnusamy,[⊥] Jamie A. S. Cleaver,[¶] Alan B. Dalton,^{*,†} Naomi E. Chayen,^{*,§} and Richard P. Sear^{*,†}

Department of Physics and Chemical and Process Engineering, Faculty of Engineering and Physical Sciences, University of Surrey, Guildford, Surrey GU2 7XH, United Kingdom, Institute of Physical Chemistry, NCSR "DEMOKRITOS", Ag. Paraskevi 15310, Athens, Greece, Department of Biomolecular Medicine, Division of Surgery, Oncology, Reproductive Biology and Anaesthetics, Faculty of Medicine, Imperial College London, London SW7 2AZ, United Kingdom, and Institute of Biochemistry, University of Lübeck, Ratzeburger Allee 160, 23538 Lübeck, Germany

ABSTRACT We report on the first use of carbon-nanotube-based films to produce crystals of proteins. The crystals nucleate on the surface of the film. The difficulty of crystallizing proteins is a major bottleneck in the determination of the structure and function of biological molecules. The crystallization of two model proteins and two medically relevant proteins was studied. Quantitative data on the crystallization times of the model protein lysozyme are also presented. Two types of nanotube films, one made with the surfactant Triton X-100 (TX-100) and one with gelatin, were tested. Both induce nucleation of the crystal phase at supersaturations at which the protein solution would otherwise remain clear; however, the gelatin-based film induced nucleation down to much lower supersaturations for the two model proteins with which it was used. It appears that the interactions of gelatin with the protein molecules are particularly favorable to nucleation. Crystals of the C1 domain of the human cardiac myosin-binding protein-C that diffracted to a resolution of 1.6 Å were obtained on the TX-100 film. This is far superior to the best crystals obtained using standard techniques, which only diffracted to 3.0 Å. Thus, both of our nanotube-based films are very promising candidates for future work on crystallizing difficult-to-crystallize target proteins.

KEYWORDS: carbon nanotubes • gelatin • nucleation • protein crystallization • nucleants • pores

INTRODUCTION

We report on the first use of carbon-nanotube-based materials to form crystals of biological macromolecules. Crystallizing these large molecules, particularly proteins, is a key problem in modern biology. Protein structures are pivotal to the success of rational drug design and to other biotechnology applications, and so international structural genomics/proteomics projects have set out to determine the structures of all of the proteins in our genome. The most powerful technique for determining the protein structure is X-ray crystallography. This, of course, requires high-quality crystals of the proteins. Producing such crystals is a very difficult task that has long been a major bottleneck to progress in structural biology. In the era of genomics/proteomics, this problem is acute: only about one in five of the proteins obtained as pure solutions have been crystallized (1). Thus, there is an urgent requirement

for new ideas and tools. Here we show that a carbon-nanotube-based material with nanometer-sized pores is an effective and versatile tool for the crystallization of proteins.

Crystallization is a first-order phase transition and so proceeds via nucleation of the crystal, followed by its growth. Without nucleation, no crystallization can occur; thus, it is important to be able to induce nucleation, and we also need to control the amount of nucleation (2, 3). This is because a common problem in crystal growth is the formation of excess nuclei, which leads to the production of large numbers of small, useless (for diffraction studies), crystals instead of the desired few large ones (1). Nucleation has only really been systematically studied for one protein, lysozyme; this is discussed in a recent review by Sear (2). For this protein, it is clear that nucleation is always or almost always heterogeneous; i.e., the crystal forms in contact with a surface (2). The situation is less clear for other proteins, although there is no reason to expect lysozyme to be exceptional. This finding of nucleation on surfaces has led to the idea of deliberately adding substances to a solution in order to provide surfaces where nucleation readily occurs. Such substances are called nucleants.

The ideal nucleant for protein crystallization should have the following properties (4):

(1) It should act as a nucleant for *many* proteins, not just one. Because proteins are diverse, this is a demanding requirement.

* Corresponding authors. E-mail: a.dalton@surrey.ac.uk (A.B.D.), n.chayen@imperial.ac.uk (N.E.C.), r.sear@surrey.ac.uk (R.P.S.). Received for review February 10, 2009 and accepted May 5, 2009

[†] Department of Physics, University of Surrey.

[‡] NCSR "DEMOKRITOS".

[§] Imperial College London.

[⊥] University of Lübeck.

[¶] Chemical and Process Engineering, Faculty of Engineering and Physical Sciences, University of Surrey.

DOI: 10.1021/am9000858

© 2009 American Chemical Society

(2) It should allow control over the number of nuclei that form, thereby promoting the growth of only one or a few crystals.

(3) The supersaturations at which nucleation occurs on the nucleant should be amenable to control, in order to nucleate crystals under conditions that are as close as possible to ideal growth conditions.

Starting with the work of McPherson and Shlichta (5), many diverse materials have been used as nucleants for protein crystallization (6–10), even including nanoparticles (11), and some success has been achieved. However, the ideal nucleant has not yet been found. Our aim was to select a novel nucleant based on knowledge of the microscopic details of nucleation. To do this, we considered the results of computer simulations. These showed that pores of size comparable to that of the nucleus (12) promote rapid nucleation. This is a generic effect that should apply to all proteins, as well as to other molecules. Proteins are a few nanometers in width, and the nucleus of a protein crystal phase is expected to be a few protein molecules in width (2). Thus, surfaces with pores ~ 10 nm in width are good candidates to induce the nucleation of protein crystals.

In earlier work, we used two types of media with nanoscale pores as nucleants: etched silicon (13) and bioglass (4). In both cases, the surfaces are composed of pores typically a few nanometers across each pore has a different size and shape. We found that bioglass induced crystallization of the largest number of proteins ever crystallized using a single nucleant (4). However, the pore sizes and surface chemistry of this particular medium are not easily controlled.

So, we sought a material with a surface with pores whose size and surface chemistry could be controlled. We found one: films of entangled carbon nanotubes (14, 15). These films are currently being investigated for a number of applications (16) because of their, for example, mechanical (17) and electrical (18) properties. We refer to these films as buckypaper. Buckypaper is a disordered mat of entangled, and typically coated, carbon nanotubes. See Figure 1. Carbon nanotubes have diameters of a few nanometers but lengths of hundreds of nanometers. Here, we present results first of the characterization of the buckypapers and then of their use as nucleants.

MATERIALS AND METHODS

Synthesis of Opaque Buckypaper with Triton X-100 (Used for All except the Results in Figure 6). Single-walled carbon nanotubes (SWNTs), synthesized via high-pressure CO conversion (HiPCO), are obtained from Carbon Nanotechnologies Inc. The buckypapers were made from a suspension of 0.04 mg/mL SWNTs and 0.4 mg/mL Triton X-100 with deionized water in a total volume of 500 mL. The TX-100 is first diluted with 40 mL of deionized water. The prepared SWNTs were then mixed with the TX-100 solution and sonicated by a probe sonicator at 28–30 W for one of two different times: 4 min ($t = 4$ min) and 40 min ($t = 40$ min). Each prepared suspension was then diluted with deionized water up to 500 mL and sonicated in a bath sonicator for 30 min. The suspension was then ready to use in the preparation of a buckypaper. The suspension was filtered through a $0.22 \mu\text{m}$ filter membrane under high pressure from a water pump. The filter was obtained

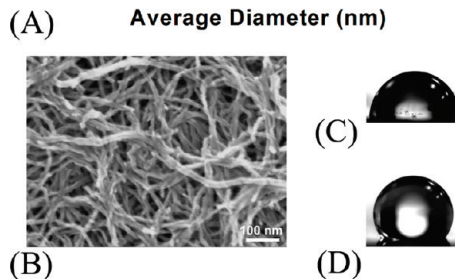
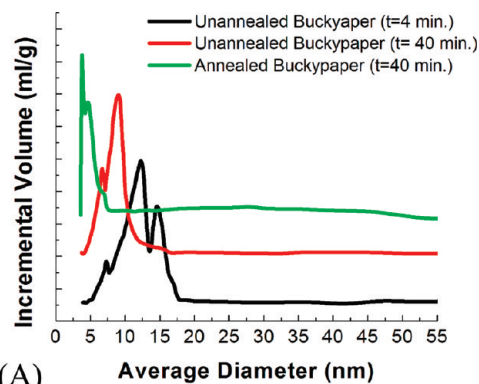


FIGURE 1. Characterization of the buckypaper made with TX-100. (A) BET pore size distributions of buckypapers. (B) SEM (Hitachi S4000) image of unannealed buckypaper ($t = 40$ min probe sonication time). (C and D) Water droplets on buckypaper for unannealed and annealed buckypaper, respectively. The contact angles are 87.6° and 114.5° .

from Millipore (a nylon filter membrane) with a diameter of 47 mm. When the entire amount of suspension was passed through the filter, 2 L of deionized water was then passed through it. The dried buckypaper was then kept in an oven at $65\text{--}70^\circ\text{C}$ for 12 h. Finally, the buckypaper was removed from the membrane by peeling it off and is then ready.

Passing deionized water through the filter removes the more labile TX-100. Note that substantial amounts of TX-100 remain to coat the SWNTs after rinsing of both preparations. The amount remaining of TX-100 was confirmed by thermogravimetric analysis (TGA) in air. We find that the buckypaper is approximately 16% TX-100 by mass.

Annealing removes the surfactant. The buckypapers, made from suspensions with a probe sonication time of 40 min, were annealed under an argon atmosphere with a heating rate of $5^\circ\text{C}/\text{min}$ and held at 600°C for 90 min.

Transparent Buckypaper with TX-100 (200 nm Thick). The suspension was prepared from dilution of 1 mL of the suspension from the probe sonication time of 40 min ($t = 40$ min) with deionized water up to 100 mL and then was sonicated with the probe sonicator at 28–30 W for 30 min and with a bath sonicator for 1 h. The suspension was then filtered through a $0.22 \mu\text{m}$ filter membrane. When the entire amount of the suspension had passed through the filter, 500 mL of deionized water was then passed through it. The dried buckypaper was then kept in an oven at $65\text{--}70^\circ\text{C}$ for 12 h. To remove the buckypaper from the membrane, the nylon membrane was dissolved in acetone. The free-standing buckypaper was attached to a cover glass.

Gelatin Buckypaper. The buckypapers were made from a suspension of SWNTs and gelatin (Sigma, porcine skin, type A) in deionized water. We started with 1 g of gelatin, which was diluted with 40 mL of deionized water and then autoclaved at a temperature of 121°C for 15 min at a pressure of 15 psi (100 kPa). The autoclaved gelatin suspension was then centrifuged twice at $3000g$, each time for 40 min. We then took the supernatant of this centrifuged suspension and added 0.01 g of HiPCO SWNTs. The resulting dispersion was sonicated at 50 W for 40 min by probe sonication. The sonicated dispersion was

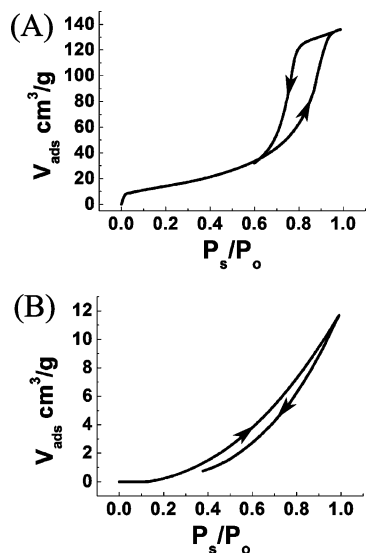


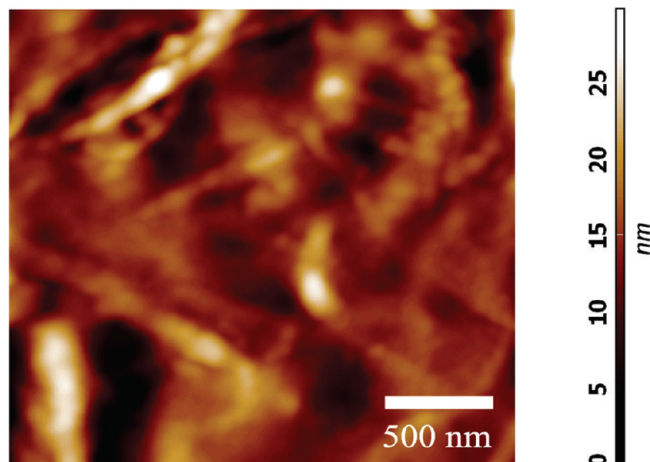
FIGURE 2. Plots of the nitrogen physisorption isotherms for (A) TX-100 buckypaper and (B) gelatin buckypaper. V_{ads} is the volume in cm^3 of nitrogen physisorbed per gram of the buckypaper as a function of the ratio of the pressure, P_s , to atmospheric pressure, P_0 . The experiment is conducted in contact with liquid nitrogen at atmospheric pressure. The upward-pointing arrows indicate the adsorption isotherm, while the downward-pointing arrows indicate the desorption isotherm. Note that in part B, although the apparent V_{ads} is actually higher for adsorption than for desorption, the difference is actually less than our estimate of the accuracy with which we can measure V_{ads} , approximately $2 \text{ cm}^3/\text{g}$. Thus, in part B, if there is hysteresis, it is too small for us to measure.

then diluted with deionized water up to 1 L and sonicated with the bath sonicator for 1 h. The suspension was filtered through a $0.22 \mu\text{m}$ filter membrane. When the entire amount of the suspension had passed through the filter, the dried buckypaper was then kept in an oven at $35 \text{ }^\circ\text{C}$ for 24 h. The gelatin buckypaper was removed from the membrane by peeling it off and is then ready.

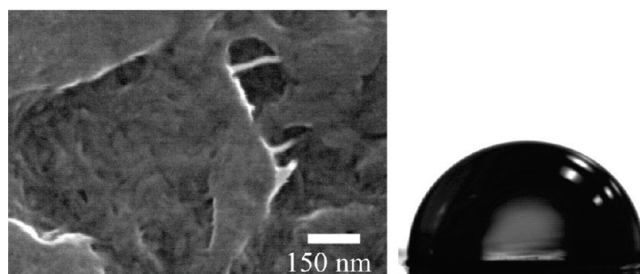
We carried out nitrogen adsorption–desorption isotherms in Figure 2 at 77 K with a calibrated Coulter series SA 3100 instrument. Standards were run before and after each buckypaper isotherm. Judging from the differences between the before and after standard isotherms, we estimate an accuracy of around $2 \text{ cm}^3/\text{g}$ in the volume adsorbed, V_{ads} , for the isotherms of our samples of mass close to 0.2 g. The Brunauer–Emmett–Teller (BET) surface area and pore size distribution in Figure 1 were obtained from these isotherms. Scanning electron microscopy (SEM; Hitachi S4000) and atomic force microscopy (AFM; NT-MDT) were both performed at the University of Surrey.

Characterization of Gelatin Solutions. Gelatin solutions were prepared as described above. To characterize the gelatin in the solution, we started with a 0.1% gelatin suspension: 1 g of gelatin in 1 L of deionized water, prepared from an autoclaved gelatin suspension as above. This suspension was stirred, by a magnetic stirring bar, for 15 min at a temperature of $70 \text{ }^\circ\text{C}$. Then, 1 mL of the warm suspension was diluted with deionized water up to 1 L. The 1 L suspension was stirred by a magnetic stirring bar for a further 15 min at a temperature of $70 \text{ }^\circ\text{C}$. Then, $10 \mu\text{L}$ of the suspension was dropped onto a cover glass (13 mm diameter, Agar Scientific), which was spun at 4000 rpm for 1 min. The surface was imaged with AFM. A typical image is shown in Figure 4.

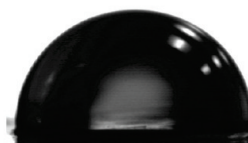
Crystallization Trials. All crystallization trials were performed using the vapor-diffusion hanging-drop method in EasyXtal Tool (QIAGEN) plates, except for the trials with transparent buckypaper. These trials used standard silanized microscope cover glasses instead of the EasyXtal Tool plates and



(A)



(B)



(C)

FIGURE 3. Characterization of the buckypaper made with gelatin. (A) AFM (NT-MDT) image of the surface of the buckypaper. (B) SEM (Hitachi S4000) image of the surface of the buckypaper. (C) Water droplet on the buckypaper. The contact angle is 89.8° .

vacuum grease for sealing. A 20 mg/mL solution of lysozyme (Sigma/L6876) was prepared by further dilution with deionized water of a 60 mg/mL solution. This solution was centrifuged at $3000g$ for 1 h and filtered through a $0.22 \mu\text{m}$ Millipore filter.

The crystallization trials with lysozyme (Figure 5A) and TX-100 (unannealed and annealed buckypapers) and gelatin buckypapers were all done in the same way, as follows. In the EasyXtal Tool plates, each reservoir contained $500 \mu\text{L}$ of a solution consisting of a 0.1 M sodium acetate (Fisher) buffer at pH 4.5 and sodium chloride (Fisher) at various concentrations. For each trial, $1 \mu\text{L}$ of a protein solution was mixed with $1 \mu\text{L}$ of a reservoir solution on a lid, which was then inverted and sealed over the reservoir. Nucleants were directly inserted into the droplets. In one experiment, five droplets were prepared at each salt concentration, and of these five, three contained the buckypaper nucleant and two did not (control droplets). The time to nucleate in this experiment, S_1 , in the presence of the buckypaper was then taken to be the average of the times that crystals were first observed in the three droplets; rare instances where in one droplet either no nucleation occurred or it occurred very rapidly were not counted. The points in Figure 5A are then the mean of five repeats of this experiment; i.e., the mean time is $(S_1 + S_2 + S_3 + S_4 + S_5)/5$, and the error bars are just the standard deviation of this set of five numbers. The control drop curve is obtained in the same way from the results obtained in the two control droplets in one set of five repeat experiments. The experiments were observed for 2 weeks.

Crystallization trials with a gelatin solution as a nucleant were performed using the EasyXtal Tool plates described above. As above, each reservoir contained $500 \mu\text{L}$ of a 0.1 M sodium

acetate buffer at pH 4.5 and 3.6% NaCl. Each control droplet was prepared by mixing 2 μL of lysozyme (20 mg/mL) with 2 μL of 3.6% NaCl. These are metastable conditions (see Figure 5A). Each sample droplet was prepared in the same way as a control droplet but with a 0.5 μL droplet of a 0.1% gelatin solution added. The experiments were observed for 1 week.

Trypsin was crystallized from a 30 mg/mL protein solution containing 20 mM Tris at pH 8.2. The reservoir solutions consisted of a 0.1 M Tris buffer at pH 8.2 and ammonium sulfate. The concentration of ammonium sulfate ranged from 1.08 to 1.32 M. At least four identical experiments were performed for each condition, with and without buckypaper.

Human cardiac myosin-binding protein-C (MyBP-C) was crystallized from a 10 mg/mL protein solution containing 50 mM NaCl and 20 mM Tris at pH 7.0. The reservoir solutions consisted of a 0.1 M HEPES buffer at pH 7.3 and poly(ethylene glycol) (PEG) of mean molecular weight 3350. The concentration of PEG 3350 ranged from 15% (w/v) to 20% (w/v) in steps of 1%. Six identical experiments were performed for each condition, with and without TX-100 buckypaper.

Approximately 10 crystals grown on the buckypaper were X-rayed at Beamline 10.1, SRS-Daresbury, using an Oxford Cryosystems cryojet at 100 K and a MAR 225 CCD detector.

Nonstructural Protein 9 of the Transmissible Gastroenteritis Virus (NSP9). The viral protein was crystallized at 20 $^{\circ}\text{C}$ from a 12 mg/mL protein solution containing 200 mM NaCl and 10 mM HEPES, pH 7.5. The reservoir solutions consisted of a 0.1 M HEPES buffer at pH 7.5, 15% (v/v) isopropyl alcohol, and PEG 3350. PEG 3350 concentrations were between 16% and 20% (w/v) in steps of 1%. Six identical experiments were performed for each condition, with and without TX-100 buckypaper.

RESULTS AND DISCUSSION

A. Buckypaper Preparation and Characterization. Two types of buckypaper were produced: one with the surfactant Triton X-100 (TX-100) and one with gelatin. Carbon nanotubes are highly insoluble in water; thus, TX-100 or gelatin is needed to coat the carbon nanotubes in order to render the surfaces hydrophilic and so disperse them in solution. Note that the gelatin buckypaper has more gelatin by mass than carbon nanotubes, and annealing the TX-100 buckypaper to remove TX-100 significantly increases the contact angle (see Figure 1C,D). So, we expect the carbon surfaces in the buckypaper to be coated by TX-100 or gelatin.

Figure 1 shows both an SEM image of a TX-100 buckypaper and pore size distributions obtained by BET analysis of nitrogen adsorption. The nitrogen physisorption isotherm is shown in Figure 2A. Note that the pores are the spaces between bundles of coated SWNTs and not the cavity within a single SWNT. From the SEM image of Figure 1B, we see that the nanotubes forming the buckypaper are not individual tubes but bundles of approximately 10 nm in width. The pore size distribution can be controlled, within a range, by varying the probe sonication time of the SWNT solution; the pores are, on average, larger if we only probe sonicate for $t = 4$ min rather than for $t = 40$ min. After $t = 40$ min, the dominant peak in the distribution of the pore sizes is around 9 nm, approximately three lysozyme protein molecules in width. The BET surface area is also a function of the sonication time. It equals 89 and 53 m^2/g for $t = 4$ and 40 min, respectively. Somewhat surprisingly, the area goes down as the pore size goes down. We only used as a

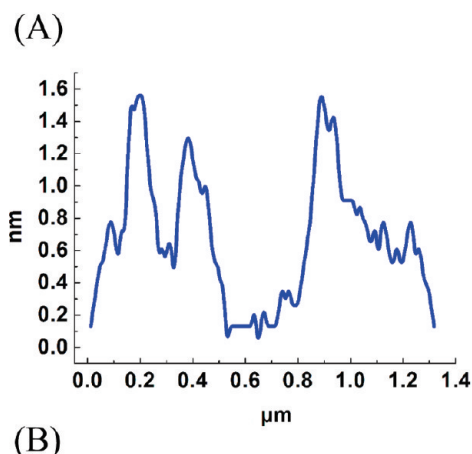
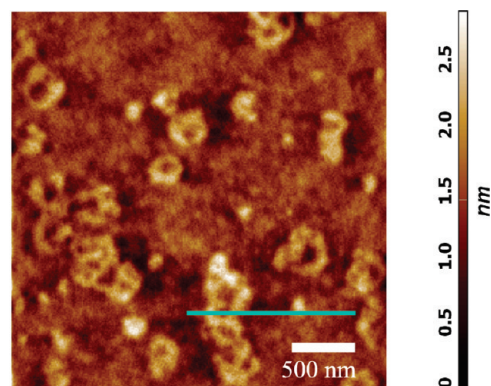


FIGURE 4. (A) AFM (NT-MDT) image of a surface that has been spin-coated with a gelatin solution. Note that the heights of the features are approximately equal to the diameter of the collagen triple helix, 1.5 nm, and that their lateral extent is typically a few hundred nanometers. (B) Height profile along the pale-green line in part A.

nucleant the TX-100 buckypaper obtained with the longer ($t = 40$ min) sonication time. In order to obtain information on the effect of surface chemistry, we also annealed some of this buckypaper in an argon atmosphere at 600 $^{\circ}\text{C}$ for 90 min. This removed TX-100 (see the Materials and Methods section), thus making the surfaces somewhat hydrophobic (see Figure 1D). It also made the pores smaller on average. After annealing, the dominant peak in the pore size distribution is at 4 nm, and the specific surface area of the annealed buckypaper is 564 m^2/g . Thus, for the buckypaper synthesized with TX-100, we have some control over both the pore size distribution and the hydrophilicity of the buckypaper, but we cannot control them independently.

Figure 3 shows an AFM height map of the surface of buckypaper made with gelatin. The much larger size of the gelatin molecules, as opposed to the TX-100 surfactant, appears to result in the spaces between the carbon nanotube bundles being filled in, or at least covered, by gelatin. We can get a clear idea of the difference between the TX-100 and gelatin buckypapers by comparing their nitrogen adsorption and desorption isotherms in Figure 2. We see that the isotherms for TX-100 have a type IV shape. This shape is characteristic of capillary condensation in mesopores. Mesopores are defined as pores of widths in the range 2–50 nm. See Sing et al. (19) for the classification scheme for physisorption isotherms. Note that the BET analysis we

employ for the TX-100 buckypaper is reasonable for type IV isotherms (only). For type IV isotherms, the initial adsorption is typically that of layers of nitrogen on the surfaces of the pores, and the large hysteresis loop is characteristic of capillary condensation in pores. Also, note that the physisorption is large, over $100 \text{ cm}^3/\text{g}$ of the buckypaper. Finally, if we place a droplet of water on top of the TX-100 buckypaper, water can percolate through to the other side. Thus, we are confident that the TX-100 buckypaper is a porous medium, which by definition contains a connected network of pores that span the complete thickness of the buckypaper.

The adsorption and desorption isotherms for the gelatin buckypaper are very different. They are close to type III (19), and the total amount of nitrogen physisorbed is 1 order of magnitude less. Also, if we place a droplet of water on top of the gelatin buckypaper, it does not percolate through. Thus, we conclude that, although the gelatin buckypaper is very rough and contains pores in the sense of deep indentations (see the AFM data in Figure 3), it is not a porous medium; it does not contain a network of interconnecting pores. It is possible that the large gelatin molecules block the pores. Below we will find that the gelatin buckypaper is a more effective nucleant than the buckypaper made with TX-100; thus, we do not require that the material be a porous medium to be an effective nucleant; a surface with roughness/pores of the right length scale is enough. Our AFM data (Figure 3) clearly show roughness, and hollows, down to length scales a little larger than the expected size of the crystal nucleus (the limit of our resolution). Thus, we expect that the nucleus of the crystal phase will feel a porelike concave surface, just as it would in our TX-100 buckypaper. This finding that a true porous medium is not required is consistent with earlier computer simulation work (12), which found rapid nucleation in model pores that were simply rectangular cross-sectional indentations.

TGA of the buckypaper showed that it contains gelatin and SWNTs in a ratio of approximately 6:4. This, together with solubilization of the SWNTs by gelatin, suggests that the surface of the gelatin buckypaper is largely gelatin. Gelatin is largely the structural protein collagen. We are not aware of any specific interactions between collagen and any of the proteins we study here. However, collagen contains charged amino acids of both signs, as well as hydrophilic and hydrophobic amino acids (20). The triple helices of collagen can also form aggregates of sizes larger than the expected nucleus size of a protein crystal and with structures on length scales from nanometers to hundreds of nanometers (21). Thus, the surface chemistry of the gelatin buckypaper is expected to be complex, and its nanoscale roughness is presumably due to the collagen fibers as well as to the carbon nanotubes. This complex surface chemistry may allow quite strong attractive interactions between the surface of the gelatin buckypaper and the crystallizing proteins. The expectation is that attractive interactions will reduce the free-energy barrier to nucleation (2).

B. Protein Crystallization Trials: Lysozyme. Having discussed the surface structure and chemistry of the

buckypapers, we present the results of our crystallization trials, first with the well-studied (23, 22) model protein lysozyme and then with the less well-studied but still common protein trypsin and finally with two difficult-to-crystallize proteins. Figure 5 presents the first quantitative results for the effect of a nucleant on the time to crystallize of a protein. The results are for crystallization of lysozyme, at $25 \text{ }^\circ\text{C}$, with 20 mg/mL protein in a 0.1 M sodium acetate buffer at $\text{pH } 4.5$. The time until the first ($5\text{--}10 \text{ }\mu\text{m}$ in width) crystal is visible is plotted as a function of the salt concentration. The crystallization conditions and protocols are described in the Materials and Methods section. The solubility of lysozyme decreases as the salt concentration increases (23, 24), so at fixed lysozyme concentration, increasing salt concentrations correspond to increasing supersaturations. At $25 \text{ }^\circ\text{C}$, tetragonal crystals coexist with a solution of approximately 20 mg/mL in the presence of 2% NaCl (24); thus, all of the salt concentrations at which we find nucleation are quite deep into the supersaturated regime. For example, at 4% NaCl, the solution at coexistence has a concentration near 5 mg/mL (24).

Crystallization is observed at NaCl concentrations down to 3.6% for the gelatin buckypaper and down to 4.4% for the TX-100 buckypaper. Both are lower than the 4.8% salt concentration, which is the lowest at which we find crystallization in our control experiments, without the buckypaper nucleant. Thus, we conclude that our buckypaper nucleants can induce crystallization at low supersaturations, at which no nucleation would occur in their absence. In addition, the buckypaper produced with gelatin is significantly more effective than that with the surfactant TX-100. At conditions such that nucleation occurred both with and without a nucleant, the time to observe a ($5\text{--}10 \text{ }\mu\text{m}$) crystal was almost the same with and without a nucleant. This suggests that when nucleation occurs, it is quite rapid and that the time to observe a crystal is largely determined by the time taken for it to grow large enough to be visible. This time is not expected to be changed by a nucleant, which is what we observe. The growth rate of lysozyme crystals is known to decrease rapidly with decreasing supersaturation (25). Interestingly, Fermani et al. (7) found that their nucleant (also based on gelatin) not only induced nucleation but greatly reduced the time taken to observe a crystal. We do not know why we find different behavior, but we do note that they used a different protein, concanavalin A, and so it is possible that the difference may be due to the different proteins.

The TX-100 and particularly the gelatin buckypapers are effective nucleants; i.e., they induced crystallization in metastable protein solutions. The ideal conditions for the growth of a well-ordered crystal are often at supersaturations that are too low to give rise to crystal nucleation. Such conditions are known as metastable, defined as those at which the drop will remain clear indefinitely if no nucleant, seed crystals, or other nucleation-enhancing procedure is

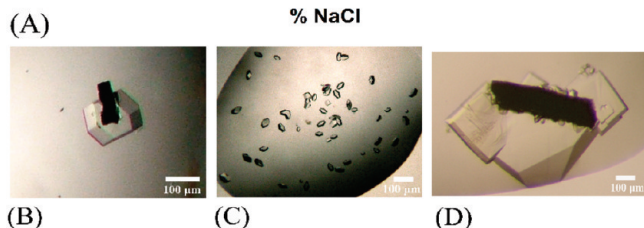
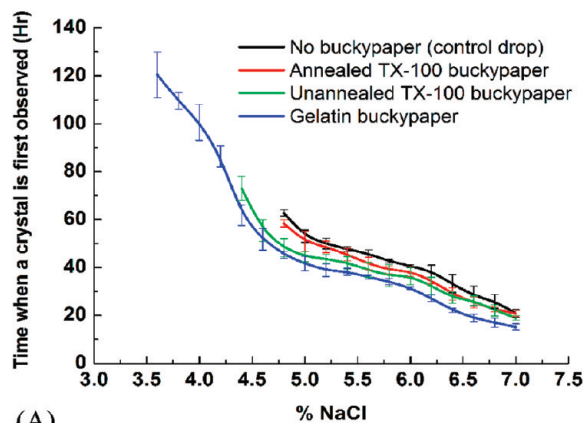


FIGURE 5. (A) Plot of the time at which a lysozyme crystal is first observed, as a function of the NaCl concentration. Crystals are 5–10 μm in width when they are large enough to be first observed. The lysozyme solution concentration was 20 mg/mL. The buffer was 0.1 M sodium acetate at pH 4.5. Each point is the average of five crystallization experiments; error bars are the standard deviations. (B) Lysozyme crystals on the gelatin buckypaper, at 20 mg/mL in 3.6% NaCl. (C) Lysozyme crystals also at 20 mg/mL in 3.6% NaCl, with a droplet of 0.1% gelatin solution added. (D) Trypsin crystals on the gelatin buckypaper: 30 mg/mL trypsin, 1.16 M ammonium sulfate, and 100 mM Tris at pH 8.2.

applied. Thus, our nucleants can be used to produce crystals at low supersaturations, allowing more ordered crystals to be formed.

Annealing the TX-100 buckypaper to remove the surfactant produced a buckypaper that is significantly more hydrophobic and has smaller pores; see Figure 1. This buckypaper was ineffective as a nucleant; adding it to the crystallization droplet did not reduce the minimum supersaturation at which crystallization occurred. Because both the surface areas and the pore sizes are changed by annealing, we cannot tell which one has the dominant effect in altering the lysozyme nucleation. It will require further systematic study to determine whether the ineffectiveness is the result of the change in the hydrophilicity of the surfaces of the pores or of the change in the mean pore size.

We found that a convenient form of the buckypaper for crystallization experiments is in small hairlike rectangular strips of 0.2 mm \times 1 mm. The data of Figure 5A were obtained with such strips. They were simply obtained using a sharp razor blade. With the gelatin buckypaper, these strips often gave too many, too small, crystals all along their length. However, this problem was easily solved by simply using a smaller piece of buckypaper; see Figure 5B. Note that there the buckypaper strip is <100 μm by a little more than 100 μm and that a large crystal has grown from it.

We also studied as nucleants both smooth surfaces coated with gelatin and gelatin in solution in order to compare their effectiveness as nucleants to that of gelatin-coated buckypaper. The trials were conducted at the lowest NaCl concen-

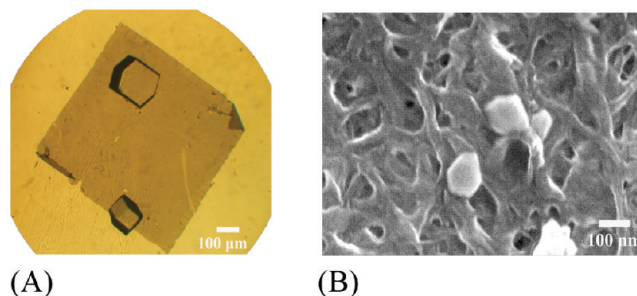


FIGURE 6. (A) Optical microscopy image of lysozyme crystals on a sheet of transparent buckypaper. (B) SEM image of a lysozyme crystal too small to be visible via optical microscopy. The buckypaper is again transparent.

tration that gave crystals with the gelatin buckypaper (3.6%). The gelatin-coated surfaces induced nucleation at low salt concentrations, as the gelatin buckypaper does; however, we found them to be difficult to use. The gelatin-coated surfaces were hydrophilic, causing the droplets to spread out, which is undesirable. Also, a large and uncontrolled number of crystals appeared. We therefore abandoned studies of these systems. We also tried mixing a dilute (0.1%) gelatin solution directly with the lysozyme and salt solution; see Figure 5C for the results. See the Materials and Methods section for details of these experiments. Here too, we found many small crystals at metastable conditions: the control droplets remained clear. The gelatin buckypaper is therefore more convenient to use and provides much greater control: it is more stable, i.e., does not have to be kept in a fridge, and by simply varying the size of the strip, we could obtain the desired few, large crystals (compare parts B and C of Figure 5, which shows the small crystals that we obtained with the gelatin solution). Many small crystals are not useful for structure determination via X-ray diffraction so for this purpose our more controllable gelatin buckypaper is better than the gelatin solution. However, gelatin solutions may still be useful for screening for conditions under which crystallization occurs, and if a solid nucleant is undesirable for some reason, then gelatin solutions may then be very useful. Fermani et al. (7) have also studied gelatin-based nucleants for protein crystallization. They studied the protein concanavalin A, and they found that their gelatin films were highly effective nucleants.

It may seem surprising that both our gelatin solutions and gelatin-coated surfaces induce the nucleation of lysozyme crystals and that a third form of the gelatin, a film, has also been found to be an effective nucleant (7). However, gelatin is largely collagen, and collagen exists as a triple helix. This has a diameter of 1.5 nm (20), is quite rigid, and aggregates in solution (forming gels at concentrations higher than those we study). A recent study of recombinant collagen by Ramzi et al. (21) found that collagen helices existed as aggregates a few hundred nanometers in width. We spun-coated surfaces with very dilute gelatin solutions and studied the gelatin on the surface with AFM; see Figure 4.

On the surfaces were aggregates a few hundred nanometers in width, and the thickness of a single collagen (triple-helix) high. In solution, an aggregate consisting of a network

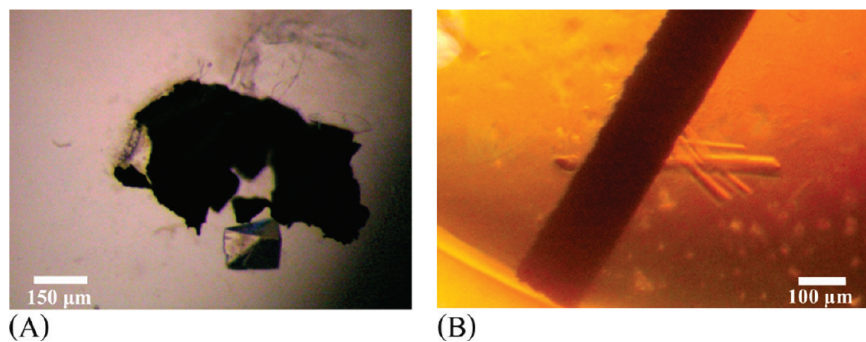


FIGURE 7. Images of crystals growing from a TX-100 ($t = 40$) buckypaper nucleant at metastable conditions. (A) C1 domain of MyBP-C. (B) NSP9.

of collagen helices would essentially be a piece of a collagen-walled porous medium a few hundred nanometers in width. The gold nanoparticle aggregates studied by Hodzhaoglu et al. (11) may likewise resemble a porous medium. Thus, our finding of nucleation due to gelatin alone, in solution as a film, or on a smooth surface is consistent with our hypothesis that materials with roughness on the length scale of the nucleus are good nucleants.

Because the buckypaper strips are smaller than the desired crystals, observing crystallization via optical microscopy is easy, despite the fact that the buckypaper is black. However, if required, large sheets of transparent buckypaper can be produced. See the Materials and Methods section for how this is prepared; we largely followed the work of Wu et al. (26). Figure 6 shows that lysozyme also nucleates on this transparent buckypaper, which is, of course, highly convenient for observing crystal growth via optical microscopy. On dried samples, we can use SEM to search for crystals too small to be visible via optical microscopy. See Figure 6B for an example. The density of such small, ~ 100 nm, lysozyme crystals on the surface of the buckypaper is relatively low, much less than one crystal per square micrometer. We do not know why the crystal did not grow larger; further study of this intriguing observation is left to future work.

C. Protein Crystallization Trials: More Difficult-To-Crystallize Proteins. Lysozyme crystallizes easily (23); therefore, we also studied the crystallization of proteins that are more difficult to crystallize, although here we were not able to obtain quantitative data on the crystallization times. We worked with trypsin (from bovine pancreas, Sigma), the C1 domain of MyBP-C (supplied by Dr. C. Redwood of Oxford University), and NSP9. Trypsin is a protease, i.e., a protein enzyme that breaks down other proteins, that is widely used in biotechnology. MyBP-C and NSP9 are both proteins relevant to human health, to cardiac disease and viral infection, respectively. The crystallization conditions are described in the Materials and Methods section. MyBP-C and NSP9, because of their scarce supply, were not tested with the gelatin buckypaper. MyBP-C was crystallized on an earlier TX-100-based buckypaper, which we used as pieces not strips.

Trypsin crystallizes spontaneously at concentrations of 1.24 M ammonium sulfate and above. At 1.20 M ammonium sulfate, crystals grew on the gelatin buckypaper within 3

days, whereas controls as well as drops with the TX-100 buckypaper remained clear for 9 days, after which crystals started appearing. At 1.16 M ammonium sulfate, crystals only grew on the strips of gelatin buckypaper, with all controls and TX-100 trials remaining clear. See Figure 5D for a crystal of trypsin that has grown from our gelatin buckypaper.

MyBP-C is a much rarer and more difficult-to-crystallize protein. However, we were able to determine that 20% PEG-3350 corresponded to a labile condition where all experiments including the controls resulted in clusters of rodlike crystals. 18% PEG-3350 corresponded to metastable conditions. There, all controls remained clear, whereas all experiments with the buckypaper resulted in crystals with various morphologies; see Figure 7A for an example. Drops with 16% PEG-3350 remained clear. Before development of the nucleant, hundreds of MyBP-C crystals were grown in clusters by conventional methods and X-rayed. The best resolution obtained from those crystals was 3.0 Å. By contrast, the best X-rayed crystals grown on the TX-100 buckypaper diffracted to a resolution of 1.6 Å, almost twice as high. It is interesting to note that in one of these drops, containing six crystals, only one of the crystals was attached to the nucleant. That was the crystal that diffracted to the highest resolution. The other crystals in that drop diffracted with a resolution in the range 2–2.2 Å. Other drops (six repeats) with nucleants present showed that in some drops the crystals were attached to the nucleant with no other crystals formed away from it, and in other drops some crystals were attached to the nucleant and others were further away from it, but in all cases, the crystals in the drops containing nucleant were single, i.e., not in clusters. All of the crystals belong to space group $I4_1$ with unit cell parameters $a = b = 48.85$ Å and $c = 95.13$ Å.

In the case of NSP9, both 19% and 20% PEG 3350 gave labile solutions, where crystals appeared in the controls as well as in the drops containing buckypaper. The buckypaper enhanced nucleation, producing showers of crystals at these conditions. The 17% and 18% PEG 3350 conditions were metastable, producing rod-shaped crystals in all of the drops that contained buckypaper (see Figure 7B), while the controls all remained clear. Drops set with 16% PEG 3350 and below remained clear. In summary, our nucleants have been shown to be effective for a range of proteins and pHs,

corresponding to crystallization conditions at pH 4.5 (lysozyme) and 7.3–7.5 (MyBP-C and NSP9). They worked with both salt and polymer precipitants.

CONCLUSIONS

To conclude, we have used materials with nanoscale porosity/roughness to control nucleation so as to obtain one or a few large crystals from solutions at low supersaturations, as is required for structure determination via X-ray crystallography. Growth at low supersaturations is expected to lead to more ordered structures, which diffract to higher resolution, and indeed this is what was found for the MyBP-C crystallized with our carbon-nanotube-based nucleants. We believe that the carbon-nanotube-based materials with nanoscale pores have great potential. The different effectiveness of our TX-100 and gelatin buckypapers implies that changing the surface chemistry and porosity changes the ability of the material to induce nucleation. Gelatin by itself was shown to promote nucleation, in accordance with a previous study (7). However, its use as a coating on the buckypaper provided a much greater degree of control over the crystallization process than when it was used either in solution or as a coating on a flat film. Carbon nanotube films made with other dispersants may be even more effective nucleants. For example, films have already been prepared using dispersants as diverse as sodium dodecyl sulfate (14, 15) and single-stranded DNA (27). These methods produce negative charges on the surfaces, which may be especially powerful for the crystallization of positively charged proteins. Finally, nanotube films may also function as nucleants for systems other than protein solutions, for example, in solutions of pharmaceuticals (28). Therefore, we believe that future work should test our materials as nucleants in other important systems where controllable crystallization is desired.

Acknowledgment. We thank Dr. Charles Redwood (University of Oxford) for providing MyBP-C and Prof. Hilgenfeld (University of Lübeck) and VIZIER (Contract No. LSHG-CT-2004-511960) for providing NSP9. We acknowledge financial support from the Engineering and Physical Sciences Research Council UK (EP/D001439/1), from the European Commission OptiCryst Project LSHG-CT-2006-037793, and

from the Thai Government for the award of a Royal Thai Government Scholarship to P.A.

REFERENCES AND NOTES

- (1) Chayen, N. E.; Saridakis, E. *Nat. Methods* **2008**, *5*, 147.
- (2) Sear, R. P. *J. Phys.: Condens. Matter* **2007**, *19*, 033101.
- (3) Gunton, J. D.; Shirayev, A.; Pagan, D. L. *Protein Condensation*; Cambridge University Press: Cambridge, U.K., 2007.
- (4) Chayen, N. E.; Saridakis, E.; Sear, R. P. *Proc. Natl. Acad. Sci. U.S.A.* **2006**, *103*, 597.
- (5) McPherson, A.; Shlichta, P. *Science* **1988**, *239*, 385.
- (6) Edward, A. M.; Darst, S. A.; Hemming, S. A.; Li, Y.; Kornberg, R. D. *Nat. Struct. Biol.* **1994**, *1*, 195.
- (7) Fermani, S.; Falini, G.; Minnucci, M.; Ripamonti, A. *J. Cryst. Growth* **2001**, *224*, 327.
- (8) Tosi, G.; Fermani, S.; Falini, G.; Gallardo, J. A. G.; Ruiz, J. M. G. *Acta Crystallogr., Sect. D* **2008**, *64*, 1054.
- (9) Thakur, A. S.; Robin, G.; Guncar, G.; Saunders, N. F. W.; Newman, J.; Martin, J. L.; Kober, B. *PLoS One* **2007**, *2*, e1091.
- (10) Sugahara, M.; Asada, Y.; Morikawa, Y.; Kageyama, Y.; Kunishima, N. *Acta Crystallogr.* **2008**, *D64*, 686.
- (11) Hodzhaoglu, F.; Kurniawan, F.; Mirsky, V.; Nanev, C. *Cryst. Res. Technol.* **2008**, *43*, 588.
- (12) Page, A. J.; Sear, R. P. *Phys. Rev. Lett.* **2006**, *97*, 065701.
- (13) Chayen, N. E.; Saridakis, E.; El-Bahar, E.; Nemirovsky, Y. *J. Mol. Biol.* **2001**, *312*, 591.
- (14) Vigolo, B.; Pénicaud, A.; Coulon, C.; Sauder, C.; Pailler, R.; Journet, C.; Bernier, P.; Poulin, P. *Science* **2000**, *290*, 1331.
- (15) Neimark, A. V.; Ruetsch, S.; Kornev, K. G.; Ravikovitch, P. I.; Poulin, P.; Badaire, S.; Maugey, M. *Nano Lett.* **2003**, *3*, 419.
- (16) Baughman, R. H.; Zakhidov, A. A.; de Heer, W. A. *Science* **2002**, *297*, 787.
- (17) Blighe, F. M.; Lyons, P. E.; De, S.; Blau, W. J.; Coleman, J. N. *Carbon* **2008**, *46*, 41.
- (18) Lyons, P. E.; De, S.; Blighe, F.; Nicolosi, V.; Pereira, L. F. C.; Ferreira, M. S.; Coleman, J. N. *J. Appl. Phys.* **2008**, *104*, 044302.
- (19) Sing, K. S. W.; Everett, D. H.; Haul, R. A. W.; Moscou, L.; Pierotti, R. A.; Rouquerol, J.; Siemieniewska, T. *Pure Appl. Chem.* **1984**, *57*, 603.
- (20) Stryer, L. *Biochemistry*, 4th ed.; W. H. Freeman: New York, 1995.
- (21) Ramzi, A.; Sutter, M.; Hennink, W. E.; Jiskoot, W. *J. Pharm. Sci.* **2006**, *95*, 1703.
- (22) Parmar, A. S.; Gottschall, P. E.; Muschol, M. *Biophys. Chem.* **2007**, *129*, 224.
- (23) Muschol, M.; Rosenberger, F. *J. Chem. Phys.* **1997**, *107*, 1953.
- (24) Cacioppo, E.; Pusey, M. L. *J. Cryst. Growth* **1991**, *114*, 286.
- (25) Gorti, S.; Forsythe, E. L.; Pusey, M. L. *Cryst. Growth Des.* **2004**, *5*, 47.
- (26) Wu, Z.; et al. *Science* **2004**, *305*, 1273.
- (27) Barsici, J. N.; Tahhan, M.; Wallace, G. G.; Badaire, S.; Vaugien, T.; Maugey, M.; Poulin, P. *Adv. Funct. Mater.* **2004**, *14*, 133.
- (28) Vairiankaval, N.; Cote, A. S.; Doherty, M. F. *AIChE J.* **2008**, *54*, 1682.

AM9000858